Life cycle assessment of the carbon intensity of deep geothermal heat systems: A case study from Scotland

Alistair T. McCay [a],[*], Michael E.J. Feliks [b], Jennifer J. Roberts [c]

[a] School of Engineering, University of Glasgow, Glasgow G12 8QQ, UK
[b] Hotspur Geothermal Ltd, 13-15 Carteret Street, London SW1H 9DJ, UK
[c] Department of Civil and Environmental Engineering, University of Strathclyde, Glasgow G1 1XJ, UK

HIGHLIGHTS

- The carbon intensity of deep geothermal heat has a lower bound of 9.7 kg (CO_{2e}) MWh_{th}.
- The carbon intensity of deep geothermal heat has an upper bound of 14.0 kg (CO_{2e}) MWh_{th}.
- Direct use geothermal heat has 7% of the emissions of gas-fired boilers.
- Deep geothermal heat is compatible with carbon reduction targets for 2050.

GRAPHICAL ABSTRACT
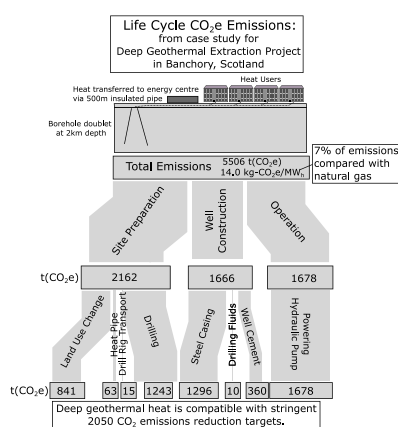
ARTICLE INFO

ABSTRACT

Deep geothermal energy is widely recognised as a source of low carbon heat. However, to date there have been no specific assessment of the carbon intensity of low-enthalpy deep geothermal; previous studies focussed on geothermal power or higher enthalpy heat. As such, there is no established method for assessing the CO_2 emissions from implementing a deep geothermal heating scheme. Here we address these gaps. We perform a life cycle assessment of greenhouse gas emissions relating to a deep geothermal heat system to (i) calculate the carbon intensity of geothermal heat; (ii) identify key factors affecting these values; (iii) consider the carbon abated if geothermal heat substitutes conventional heating; and (iv) present information that future projects can apply to assess the carbon emissions reduction offered by geothermal heat development. Our work is informed by parameters from a feasibility study for a proposed geothermal heat system in Banchory, Scotland. The project planned a 2.5 MW_{th} geothermal plant extracting heat from the Hill of Fare granite via two boreholes, one injection and one production. We find that the majority of the emissions are associated with site construction, and sensitive to site and materials specific factors, for example the depth of the drilled boreholes and type and quantities of steel and cement used to seal them, or soils disturbed for laying pipelines and constructing access roads. During operation the carbon intensity of the electricity grid used to power hydraulic pumps largely determines the carbon intensity of the produced heat. We calculate that the carbon intensity of the heat produced is 9.7–14.0 $kg(CO_{2e})$ MWh_{th}

which is 4.9–7.3% of the emissions from heat from natural gas. These values are compatible with Scotland's plans for long term decarbonisation of heat in line with national emission reduction obligations and would likely be compatible with any country's decarbonisation goals.

1. Introduction

1.1. Heat energy and carbon emissions

There is international consensus, recognised by The Paris Agreement (UNFCCC, 2015), that global reductions in greenhouse gas (GHG) emissions are urgently required to prevent dangerous climate change. The most important GHG produced by human activity is CO_2, and successive UK and Scottish Governments have set ambitious targets for reduced CO_2 emissions. In colder, northern European countries, more CO_2 emissions typically arise from the demand for heat than from the power or transport sectors; in the UK 38% of CO_2 emissions were estimated to be related to heat in 2009 (DECC, 2012). Space heating in public and private building represents the largest part of this demand and is often met via fossil fuel heat technologies. In Scotland 80% of households use natural gas for heat, overwhelmingly via individual boilers (Scottish Government, 2018). Identifying practical options for decarbonising the heat sector at scale must therefore be an important element of any nation's strategy to deliver significant reductions in their national greenhouse gas emissions.

Life cycle assessments (LCAs) of greenhouse gas emissions are often used to inform the relative merit of low carbon alternatives. They allow comparisons to be made between different approaches under a national decarbonisation strategy by identifying where emissions could be reduced through, for example, technological development or changes in practice (European Commission, 2010). LCAs usually present a full assessment of the direct and indirect emissions of GHG expressed as CO_2 equivalent (CO_2e). For energy resources it is conventional to express the carbon intensity of a fuel in terms of the total GHG emission per unit of energy. This value represents the total emissions associated with project development and operation amortised over the total amount of energy produced during the project lifetime.

One promising potential source of low carbon heat is deep geothermal energy, which utilises the heat found in deep rock strata to meet heat demands at the surface. The technology to do this is well established, though has largely been applied in regions with 'high enthalpy' volcanic geothermal resources (e.g. Iceland, New Zealand). Water is invariably used as the medium to transfer heat from depth to surface. While producing electricity from geothermal resources requires high temperatures and advanced turbines, producing direct heat is relatively straightforward and could potentially be deployed in a wide variety of geological settings. Locations such as Paris, France (Vernier et al., 2015), the Netherlands (Van Heekeren and Bakema, 2015) and parts of China (Lund and Boyd, 2016) have significant geothermal heat production rates with markets at various levels of maturity.

Deep geothermal heat generation is generally considered to be a low carbon resource (Gluyas et al., 2018). However, to date there have been few studies assessing its carbon intensity and the factors affecting it. Karlsdottir et al. (2014) studied a district heat system in Stykkishólmur, Iceland, where brine at 70 °C is extracted from a borehole drilled at a distance of 5 km from the town (i.e. the heat users). The study finds that the carbon intensity of the heat is 5.8 kg(CO_2)/MWh$_{th}$, and the majority (64%) of these emissions comes from the geothermal heat production. However, this value includes the installation and operation of the town's district heat network as well the pipework needed to transport the heat from the boreholes to the heat network, which limits how usefully the study can be applied to appraise options for supplying heat to district heat networks. Pratiwi et al. (2018) modelled the carbon intensity of heat produced from an enhanced geothermal system in the Upper Rhine Valley which extracts brines at 170 °C. A heat-only scenario estimates a carbon intensity of 9.15 kg(CO_2)/MWh$_{th}$, over 1/3rd greater than estimates from Karlsdottir et al. (2014). In this paper, we assess the carbon intensity of heat produced from a region with a relatively low geothermal gradient (i.e. <120 mW/m^2). For geothermal heat to make a significant contribution to heat decarbonisation over a broad geographical area, it will be important to exploit low-enthalpy resources, otherwise the technology will be restricted to the limited areas with a naturally high geothermal gradient. Not only does this study present the first LCA of low-enthalpy heat systems, it also presents a methodology to assess the potential reduction in CO_2 emissions that could be achieved by implementing a deep geothermal heating scheme which can be adapted for different settings.

There is comparably more published work that aims to calculate the carbon intensity of geothermal *power* (not heat). These studies find a wide variation in emission intensity due to operational and geological variances. Bruckner et al. (2014) assume the carbon intensity of geothermal power is in the range 6–79 kg(CO_2e)/MWh$_e$, with a 50th percentile figure of 45 kg(CO_2e)/MWh$_e$. This places geothermal energy in the range of renewable energy generation (solar PV is 46 kg(CO_2e)/MWh$_e$, offshore wind is 12 kg(CO_2e)/MWh$_e$, and for comparison the carbon intensity of power from natural gas and coal is 469 and 1001 kg(CO_2e)/MWh$_e$ respectively). Other estimates have been higher. For example, Bertani and Thain (2002) reviewed the carbon intensity of deep geothermal power plants worldwide and report an average of 122 kg(CO_2e)/MWh$_e$. However, reported values varied greatly for a typical power plant in different countries. For example, geothermal power plants in Iceland have an average of 34 kg(CO_2e)/MWh$_e$ whereas plants in Italy are a magnitude greater, at 330 kg(CO_2e)/MWh$_e$ (Fridriksson et al., 2017) and deep geothermal plants in Turkey may be as high as 1800 kg(CO_2e)/MWh$_e$ (Aksoy et al., 2015). The emission intensity varies so widely because geothermal power plants tend to tap volcanogenic derived fluids, which are typically naturally rich in CO_2. These gases may be vented or emitted as part of power production. Further, geothermal power generates significant amounts of heat as a by-product, which is rarely utilised. Deep geothermal heat production, as opposed to power production, can be a more efficient process as the vast majority of heat produced can be used, and with (generally) closed loop systems CO_2 venting does not occur. As such, geothermal heat exploitation, which generally targets mid to low enthalpy systems which are not volcanogenic, do not have such excessive associated CO_2. The carbon intensity of low enthalpy deep geothermal heat production is therefore expected to be significantly lower than for geothermal power, but more evidence is required to determine just how much power.

Here for the first time we conducted an LCA to estimate the carbon intensity of a low-enthalpy deep geothermal heat generation. To inform our work, we adopt parameters from a feasibility study for a deep geothermal heat project in Banchory, Scotland (Milligan et al., 2016).

1.2. The Banchory Geothermal Project

The geothermal potential of Scotland remains to be fully understood but is generally divided into two geological settings. The first is the hot sedimentary aquifers which are likely to exist below the Central Lowlands (e.g. Comerford et al., 2018), while the second is the large granite plutons of the North East where heat is generated through decay of radioelements. The Hill of Banchory Geothermal Feasibility Study (Milligan et al., 2016) explored the scope for a geothermal heat system in Banchory, a town 25 km west of Aberdeen (Fig. 1). The town sits just
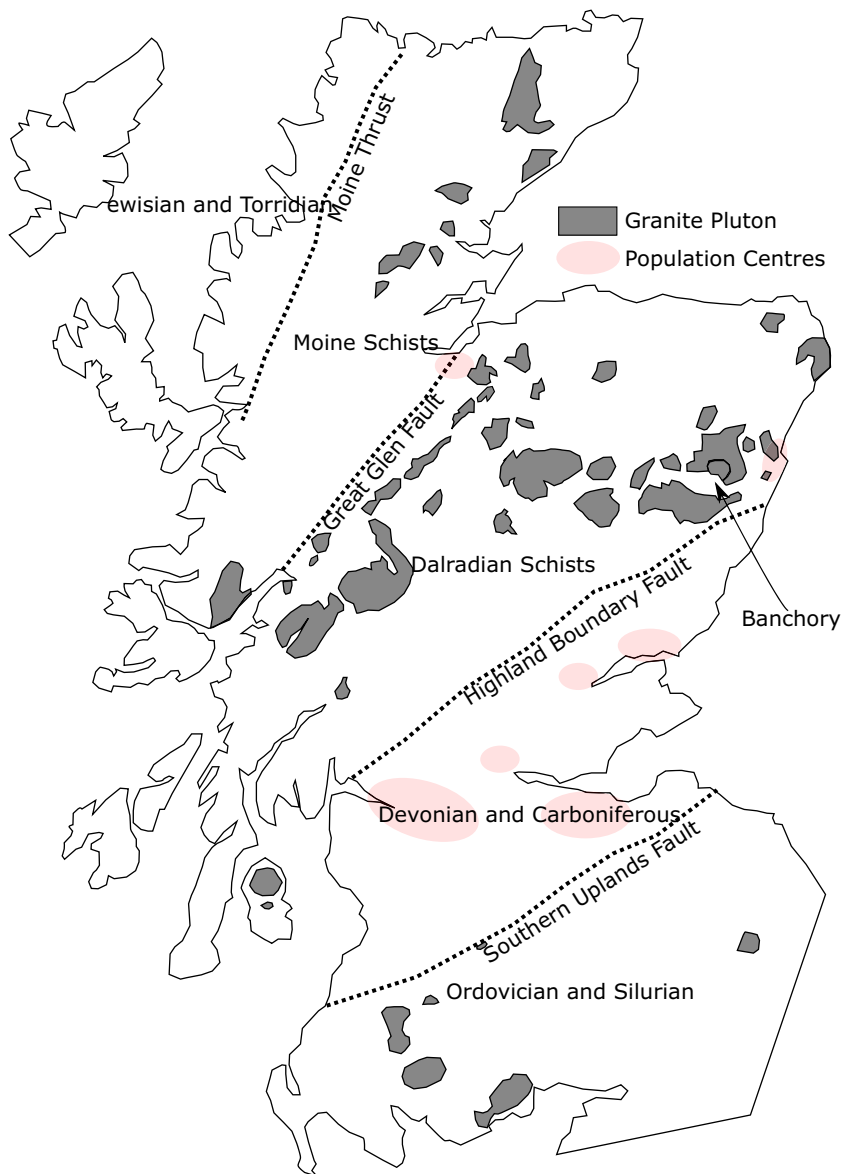
Fig. 1. Simplified map of Scotland showing the location of The Hill of Banchory Feasibility Study, the main geological terrains, the location of granite plutons (dark grey), and the location of Scottish cities (pale pink). (For interpretation of the references to color in this figure legend, the reader is referred to the web version of this article.)

south of the Hill of Fare granite pluton and already has a small heat network (currently using biomass fuel) which could accept geothermal heat and allow the network to meet the expected rise in heat demand in the town.

The town of Banchory in Aberdeenshire (Scotland) was a site of a deep geothermal heat feasibility study for two reasons:

Firstly, gamma ray spectrometry surveys had identified the Siluro-Devonian Hill of Fare granite, located 2 km North of Banchory, as a potential heat resource due to its elevated concentration of radioelements (McCay and Younger, 2017). No boreholes have been drilled at the Hill of Fare, but the feasibility study's estimation was that temperatures of between 65 °C and 82 °C – enough to provide space heating – would be found at a depth of 2000–2500 m. There was no estimate of the hydraulic conductivities for the Hill of Fare granite due to a lack of required geological information. Instead, Milligan et al. (2016) used comparative studies of similar projects in granites to produce high, medium, and low flow scenarios.

Secondly, Banchory's district heat network needed to expand to meet the towns growing heat demand. The town's current population

is ~7500 (Aberdeenshire Council, 2016), but the population is increasing and planned new residential districts offered scope for the existing energy supply company to use geothermal heat to meet baseload heat demands (the existing biomass system would be used to meet peak loads).

2. Assumptions and methodology

This section sets out and explains the activities involved in the key stages of a direct heat geothermal project, as well as the assumptions that we adopt to estimate the carbon intensity of each stage. We present this in line with ISO 14040:2006 to facilitate comparison with other life cycle studies.

2.1. Goal and scope

The goal of this study is to estimate the whole life cycle climate impact of direct heat production from low-enthalpy deep geothermal projects, where low-enthalpy refers to temperatures <90 °C (e.g. Tavman et al., 2005) and deep is defined in UK law as deeper than 500 m

below ground (Ofgem, 2014). This information will be used to inform three main objectives:

- quantify emissions for low-enthalpy deep geothermal in terms of kg $(CO_2e)/MWh_{th}$;
- analyse which processes are responsible for the majority of emissions, and where carbon reduction efforts could be focussed; and
- establish the extent to which low-enthalpy deep geothermal is compatible with long term, stringent, decarbonisation pathways.

The Hill of Banchory Geothermal Feasibility Study (Milligan et al., 2016) was funded by the Scottish Government's Low Carbon Infrastructure Transition Programme (LCIPT). The study identified an optimum design for the project. This comprised two directionally drilled boreholes (one for production and one for injection, i.e. a 'doublet' system) plus surface water piping from the granite pluton to an energy centre (outlined in Fig. 2) located 1 km from the Banchory district heat network. Each borehole would have 2 km horizontal reach and 2–3 km vertical reach, and the production and re-injection boreholes would operate as a sealed system. We refer to the proposed design as the 'Banchory Project'. Note that the Milligan et al. (2016) concluded that the Hill of Fare geothermal heat source was not commercially viable, not because of any technical issues relating to the geothermal system, but simply because the district heat network had access a ready supply of biomass fuel which could offer more carbon emissions reduction at lower cost.

Our study considers the emissions associated with the development and operation of the geothermal project, from site preparation until decommissioning. Decommissioning is not included since the decommission activities largely depend on how the site is re-purposed, and this is decided towards the end of the project life. We also do not consider the emissions associated with servicing and maintaining the well, since this may not be needed, and if it is, the carbon emissions associated will be variable depending on the necessary activities.

The project lifetime was estimated by Milligan et al. (2016) to be 30 years, which is in-line with other deep heat-only projects (for example, Pratiwi et al. (2018) estimated a 25 year lifetime while Frick et al. (2010) estimated 30 year lifetime for deep geothermal heat, both studies were based in Germany). Fig. 3 shows the scope of our LCA and the required materials and main waste streams that we evaluate in terms of the CO_2 equivalent emissions per unit of heat, expressed as kg $(CO_2e)/MWh_{th}$.

2.2. Inventory analysis

This section details the main processes involved in the construction and operation of the Banchory Project, and the assumptions made about these processes. Table 1 summarises the key parameters adopted to inform the life cycle assessment, the underpinning assumption and the information source. Each of the steps in Table 1 is explained further in the subsections that follow.

2.2.1. Construction of the geothermal system

The site construction stage includes the preparation and construction of surface infrastructure including the well pad, access roads and delivery or distribution facilities, and the drilling and completion of the boreholes.

2.2.1.1. Land use change. The carbon content of soil can vary hugely. For instance, peat soil contains high levels of carbon (>50–60% carbon) whereas arable mineral soil has a very low level of stored carbon. When infrastructure is built upon these soils, the use of that land is changed. This can cause the soil carbon to be released as CO_2 through the oxidisation of the organic materials (Oertel et al., 2016). Furthermore, photosynthesis opportunities may be lost for that area of land (Bond et al., 2014). Land use change can be a significant source of CO_2 emissions for new energy developments, particularly if carbon rich soils, such as peat, are disturbed (Nayak et al., 2010). The type of soil and excavation area will ultimately determine the amount of carbon being released as a result of land use change.

For geothermal resource development, land may be cleared for well pad construction and service supply. The well pad is where the drilling and other subsurface operations take place, and so roads and possibly pipelines service these. To calculate the emissions from land use change we follow the method of Bond et al. (2014).

To construct the well pad, the top soil is removed to reveal the subsoil, the excavated surfaces are compacted, and then a concrete blinding pad is prepared. Reinforced masonry bunds must be built to protect inundation from flood events or to prevent chemical spillage from polluting the surrounds. The bunding requirements would be site specific.

For the Banchory Project we assume that the area cleared for a drilling-only well pad would be ~0.75 ha to a depth of 0.25 m. This is in line with the parameters proposed for exploration drilling for any well. In total, 1875 m^3 of soil is disturbed (i.e. removed and oxidised) for the well pad. We assume that a short (200 m in length) access road will be built to access the energy station from the nearest paved road. Single track access roads are assumed to be ~6.54 m width, and land will typically be excavated to 0.3 m depth to lay the road on well-drained soil (Ryan et al., 2004). In total, 392.4 m^3 of soil is removed and oxidised for the access road, which is rounded to 400 m^3 in our calculations. The total land area affected by the well pad and the access road is ~0.9 ha (xx m^2). The carbon loss from terminating photosynthesis processes after the soil is disturbed is assumed to be negligible.

We assume that the heat pipelines would be insulated and buried, since this is standard practice. Often, pipelines are laid together to minimise land disturbance and cost, and for ease of maintenance. While the surface area of land disturbed to lay the pipeline will be minimal, a volume of soil is removed to lay and bury the pipe. It is industry standard to bury pipelines to minimum depth of 1.1 m below surface, and involved excavating soil to approximately 1.4–1.5 m depth, laying the pipes and cables, and replacing the soil. It is expected that the topsoil will regenerate back to its original state relatively quickly in the UK environments, and generally within 1 year. The amount of soil permanently excavated to lay the pipelines is equivalent to the volume of the pipes and cables.
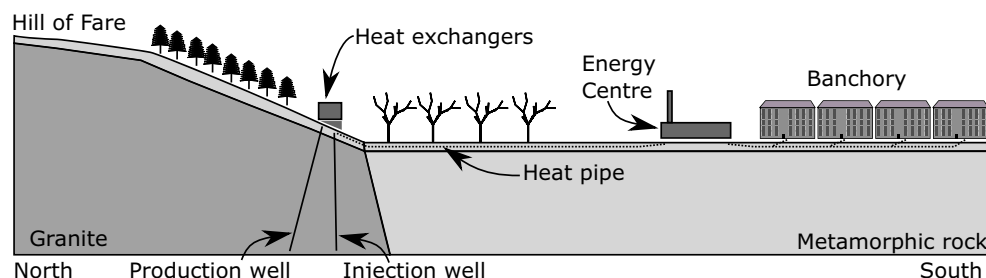

Fig. 2. Schematic of the Banchory Project which we use as case study for our life cycle analysis of low enthalpy geothermal heat systems.
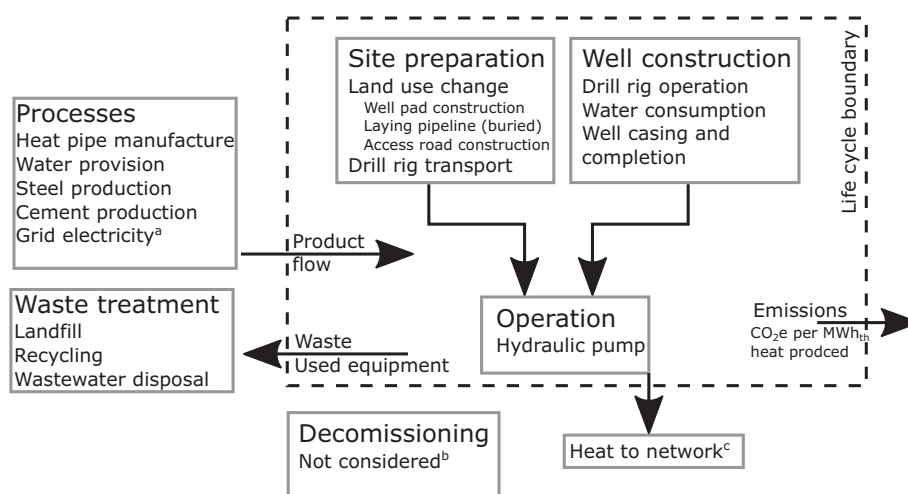
Fig. 3. System boundary for our life cycle analysis, depicting the main input and output components and the processes considered. Note: a) The carbon intensity of grid electricity is assumed to decrease over the project lifetime, reducing from the current UK average of 280 kg(CO_2e)/MWhe (BEIS, National Grid Data, 2018) to <100 kg(CO_2e)/MWhe in line with national strategy (Committee on Climate Change, 2018). b) Emissions associated with decommissioning are not considered here as they depend on how the site is re-purposed following the project close. c) Heat is assumed to be supplied to a district heat network that is already constructed (as is the case for Banchory). For projects with no heat network already in place, additional emissions from the sourcing and construction of the heat network may need to be included in the full life cycle footprint.

We assume pipeline width of 0.4 m, and insulation of 0.1 m (5 cm thick around the outside of the pipe), leading to total conservative pipeline diameter 0.5 m. As such, for 2 km of buried pipe, 392.7 m^3 soil is removed and oxidised, rounded to 400 m^3 for calculation.

Soils around Banchory are arable, wooded, or heather (UK Soil Observatory, 2007). Woodland would not likely be cleared for energy development, and so we assume that the energy station, well pad and roads would be developed on either arable or heath. These soils have carbon density values of 35.19 ± 4.89 and 295.49 ± 16.53 kg/t, and soil bulk density values of 1.16 and 0.29 t/m^3 respectively. The UK Soil Observatory reports values for the top 15 cm of soil, whereas the standard carbon inventory default depth is to 30 cm (Ward et al., 2016). Further, the carbon content of arable mineral soils and grassland are not constant with depth; carbon content decreases with depth. To account for this, we adopt an average value to represent the carbon content for each soil type. For grasslands, the greatest concentrations of total carbon (% total C) are in surface soils to 7.5 cm depth (Ward et al., 2016), and soil bulk density also increases with depth. We assume that the carbon content of the soil is approximately half of the carbon density reported for the top soil. This is likely to be a conservative estimate.

The land use activities described above results in the removal and oxidation of a total of 2675 m^3 (1875 m^3 for well pad, 400 m^3 for roads, and 400 m^3 for pipelines). As a lower bound, if we assume all this land is arable then 108 t(C) will be oxidised resulting in the release of 400 t(CO_2e). As an upper bound, we assume all this land is heath then 228 t(C) will be oxidised resulting in the release of 841 t(CO_2).

2.2.1.2. District heat pipes. Higher temperature (80 °C) district heating pipes are constructed from pre-fabricated insulated steel sections. Plastic can be used in place of steel at lower temperatures. We assume that the 1 km delivery/return pipes (2 km pipe length in total) that connect the boreholes to the energy centre will be insulated steel of 100 mm diameter (DN 100). Fröling et al. (2004) calculate that the embedded carbon within a 12 m section of such pipe would be equivalent to 380 kg (CO_2), of which 240 kg is associated with the steel. A 2 km section of pipe therefore represents 62 t(CO_2) embedded CO_2.

Table 1
Key parameters and assumptions in the life cycle assessment, based on the Banchory Project parameters and other published data, structured to reflect the chronological development of project activities.

Parameter	Assumption			Source
1. Construction				
a) Site preparation				
Area of well pad	0.75 ha			Bond et al. (2014), Milligan et al. (2016)
Access road	0.15 ha (200 m access road at 6.5 m width)			Bond et al. (2014), Milligan et al. (2016)
Pipework	1 km of buried delivery-return pipe, 0.5 m diameter			Milligan et al. (2016)
b) Borehole construction	Standard scenario	Favourable drilling scenario	challenging drilling scenario	
Vertical depth (per well)	2000 m	1800 m	3000 m	Milligan et al. (2016)
Drill rig diesel consumption	3785 l/day	3785 l/day	3785 l/day	Bradley (1987)
Drilling time per well	1500 h	1200 h	3000 h	Milligan et al. (2016)
Drilling water consumption (per well)	5000 m^3	4500 m^3	10,000 m^3	Bond et al. (2014), MacKay and Stone (2013)
Steel casing (per well)	2000 m	500 m	3000 m	Milligan et al. (2016)
Cement (per well)	200 t	180 t	400 t	Ng'ang'a (2014)
2. Operation				
Production pump power	14–28 kW			See Section 2.2.2
Injection pump power	0–28 kW			See Section 2.2.2
Project lifetime	30 years			Milligan et al. (2016)
Well servicing	Not considered			
Heat capacity	2.5 MW$_{th}$			Milligan et al. (2016)
Load factor	60%			See Section 2.2.3
Heat production (annual; lifetime)	13,140 MWh$_{th}$; 394,200 MWh$_{th}$			See Section 2.2.3
3. Decommissioning	Not considered			

2.2.1.3. Drilling and preparing the borehole. The time taken and the resources required to drill boreholes is highly variable, and largely depends on the properties of the geological formation being drilled. To test the sensitivity of carbon emissions to the parameters assumed for drilling the geothermal wells we developed three drilling scenarios (shown in Table 1). The "standard" scenario was based on best estimates from the Banchory Project; the "favourable" scenario encounters high-end temperatures and favourable ground conditions, and the well takes −20% less time than the standard scenario; and the "challenging" drilling scenario considers a prolonged drilling programme, in which the time taken to drill the well is twice the length of the standard scenario. These difficulties could be caused by unexpectedly low temperatures, particularly hard rocks, regular loss of drill fluid, or technical mishaps such as losing a drill bit (as happened at the Science Central Borehole in Newcastle, which required a retreat and additional drilling (Younger et al., 2016)).

We assume that one drill rig is transported to site to drill the two boreholes and adopt emission values for rig transport reported in MacKay and Stone (2013). We assume that the rig is powered by diesel because, while rigs powered by natural gas or electricity are available (King, 2012), they are not yet industry standard. The fuel consumption of the engines that power the drill rigs vary based on their size and engine efficiency. Here we assume 3785 l/day (157.7 l/h) diesel consumption after Bradley (1987) information on typical hydrocarbon drilling. Our standard drilling scenario assumes that drilling a 2000 m borehole in granite will take ~1500 h (236,500 l/well diesel consumption). This time estimate is based on the experience of comparable boreholes, for example the 1800 m Science Central geothermal borehole (Younger et al., 2016) beneath Newcastle (UK) was drilled in two phases over ~1700 h. We calculate emissions from drilling by assuming that diesel combustion produces 2.63 kg(CO_{2e})/l of fuel. We do not account for the CO_{2e} emissions of other pollutants that source from diesel combustion, such as black carbon.

Drilling requires large amounts of liquid for lubrication, and typically drilling mud is used to circulate cuttings within the borehole. In line with other work (e.g. Forster and Perks, 2012) we do not consider emissions from sourcing bentonite for drilling mud. We account for drilling water following the approach of MacKay and Stone (2013) we assume that a maximum of 5000 m³ of water is used per well for drilling. However, we acknowledge that water usage could be much greater, particularly if the granite has permissive fractures, so we double this amount to 10,000 m³ for the challenging drilling scenario. Indirect CO_2 emissions for water consumption and for water treatment and disposal are 0.34 kg(CO_{2e})/m³ and 0.71 kg(CO_{2e})/m³ respectively (DEFRA, 2018).

Geothermal boreholes will be fully cased and cemented as standard, although a borehole directly in granite may only be needed to be cased to ~30 m (Milligan et al., 2016). The Banchory well design used 17 1/2″ casing to ~100 m, then 13 3/8″ casing to ~500 m, then 9 5/8″ diameter casings to line the production zone. We adopt this as the standard design assuming the production zone begins at 1800 m. For the favourable drilling scenario, we assume the boreholes are fully cased to 1000 m with rock strength integrity allowing no casing beyond that. The challenging drilling scenario assumes that we fully cased the boreholes to 3 km. We calculate the embedded carbon in the steel of the casing using an upper bound estimate of Yu et al. (2015) and WorldSteel (2016) of 2.7 t(CO_{2e})/t(steel), assuming that the casing weighs no >100 kg/m (ISO 11960:2014). We note that this only accounts for the raw material and so does not include the emissions embedded from casing manufacture and transport. To seal the borehole, we estimate, following Ng'ang'a (2014), that 200 t cement would be used per borehole in the standard scenario, 180 t per borehole for the favourable drilling scenario and 400 t per borehole in the challenging drilling scenario. We assume ~900 kg(CO_{2e})/t for cement produced by current practices (Salas et al., 2016) and without any chemical additives.

The embedded carbon associated with surface hardware, including the pump, heat exchanger and so on are not accounted for here, since they are deemed to be minimal (c.f. the carbon emissions involved in manufacturing several mid-size cars are around 15 t(CO_{2e}) (Sullivan et al., 2010)). Further, we do not consider the district heating scheme infrastructure at the potential Banchory project because (a) it is already in place and (b) any comparable heat source (gas, biomass, heat pump etc.) would require this infrastructure to be in place, and so these embedded emissions are not unique to deep geothermal heat sources.

2.2.2. Operating the scheme

We assume that the lifetime of a deep geothermal system at Banchory would be 30 years, for reasons previously provided. Geothermal heating systems can last much longer (for example, the geothermal heat system in Boise, Idaho has been in operation since the 1890s), however the lifetime will be dependent on local factors such as the rate of decline in flow rate (which will be accelerated if the pumped output from the borehole is too high or the rate of the accumulation of fines in the pipes - a problem for the geothermal systems in Paris).

During the project lifetime some refurbishment of the system such as occasional pump replacement or de-scaling will be necessary. However, scaling is usually only an issue during large temperature drops such as the 90 °C drop in the ORC tube heat exchanger at the Soultz-sous-Foret geothermal project (Scheiber et al., 2013). As such, we do not account for these activities in this work.

There would be no CO_2 or CH_4 venting during heat production at the Banchory project: The Hill of Fare granite pluton is not a volcanic geothermal source, and it is proposed that the production and re-injection boreholes will operate as a sealed system.

During the operation of the geothermal system the dominant energy input is the electrical power to the pump that circulates the produced and injected fluids. We assume this will operate using grid electricity, rather than a gas- or diesel-powered generator. The thermal fluid will not need to be pumped from the full depth of the borehole since artesian pressure will raise the level of water in the borehole to the level of the local water table, a point much nearer to the surface (cf. Younger and Manning, 2010; Hogarth and Bour, 2015). This greatly reduces the work that must be done by the pump.

However, since the hydrostatic head of the fracture systems at depth isn't known for the Hill of Fare granite, it is difficult to make a robust calculation of the work done by the pump, and thus the CO_{2e}/MWh$_{th}$ of heat generated. In the absence of this information, to give indicative figures for the power consumption we calculate the power required to raise water from minimum and maximum heads, which we take to be $h_{min} = 50$ m and $h_{max} = 100$ m below ground level based on experience of drilling in UK granite from Younger and Manning (2010).

We assume the pumping rate is approximately 0.02 m³/s, and industry standard pump efficiency of 0.7, or 70%. We then calculate the pump power using the h_{min} and h_{max} figures for the pumping heads using Eq. (1), which gives the power used by the pump:

$$P = \frac{\rho \, g \, Q \, h}{\eta} \tag{1}$$

where P = power (W); ρ = fluid density (kg/m³); g = gravitational acceleration (m/s²); Q = pumping rate (m³/s); h = pumping head (m); and η = the efficiency of pump.

The estimated pump power ranges from 14 to 28 kW, which is in agreement with other geothermal developments such as 20–40 kW at Soultz-sous-Foret (DECC, 2013). Gravity recharge is a preferred method of reservoir reinjection. However, the use of reinjection pumps can be necessary. We therefore double the power requirement of the upper bound estimate to 56.1 kW, to account for a 'worst case' scenario where reinjection pumping is required. A 60% load factor equates to annual power consumption between 74 MWh$_e$ and 294 MWh$_e$. The CO_2 footprint of operating the pump is dependent on the carbon intensity of the grid supply. Currently in the UK this is 280 kg(CO_{2e})/MWh$_e$ supplied (BEIS, National Grid Data, 2018), and so the pump operation

equates to 21–83 t(CO_2e)/Pa. However, over the project lifetime the carbon intensity of the UK grid is expected to decrease significantly to <100 kg(CO_2e)/MWh$_e$ in 2030 (Committee on Climate Change, 2018). For this work, we assume that the grid carbon intensity falls steadily over the lifetime of the Banchory project, from current values (max) to 100 kg(CO_2e)/MWh$_e$ (min). In other words, we take the average carbon intensity of power taken from the grid over the plant's operation to be 190 kg(CO_2e)/MWh$_e$.

2.2.3. Decommissioning

At the end of the project lifetime the site could be decommissioned, if not repurposed for continued geothermal exploitation. This includes plugging and abandoning the injection and production wells by filling the well with cement then cutting the well below the surface so there is no surface footprint. All equipment and waste would be removed, including the well pad and access roads (unless the land owner requests that the infrastructure remains), and the land must be returned to the same conditions, or better conditions, than it was prior to the construction of the exploration borehole (SEPA, 2012).

Previous LCAs for energy developments do not consider the emissions related to well plugging and site restoration activities because data are sparse (MacKay and Stone, 2013; Bond et al., 2014). For the Banchory site, the main source of emissions would be from the concrete infill to seal the borehole, with some negligible emissions from infrastructure removal and site restoration (Bond et al., 2014).

2.2.4. Heat produced

The capacity of a geothermal borehole doublet at Banchory was expected to be 2.5 MW$_{th}$ of heat and would have a load factor of 60% (Milligan et al., 2016). Over thirty years the total heat generated by the system therefore amounts to 394,200 MWh$_{th}$.

3. Results

The estimated direct and indirect carbon emissions for each step of the life cycle for the Banchory deep geothermal heat project are shown in Table 2 and Fig. 4.

We find that the majority of the emissions are associated with pre-operation stage, and so are sensitive to site specific factors (borehole depth, pipeline length, water consumption while drilling, drilling duration), and material specific factors (cement or steel properties) or the area and type of soils disturbed for laying pipelines and constructing access roads (in this case, heather or arable land). During the project's operation, the pump rate and the carbon intensity of the electricity grid (used to power the pump) determines the carbon intensity of the produced heat. Overall we find that the total carbon intensity of the produced heat is in the range 9.7–14.0 kg(CO_2e)/MWh$_{th}$ for the standard scenario. The favourable drilling scenario (1.8 km deep well) has range of 7.8–12.1 kg(CO_2e)/MWh$_{th}$, whereas the challenging conditions scenario (4 km deep well) shows a range of 15.4–19.7 kg(CO_2e)/MWh$_{th}$. The upper and lower bounds depend on the land use and the pump rate for the project lifetime, as well as the assumed percentage load factor of the system.

4. Discussion

4.1. Key factors and sensitivities for carbon intensity of geothermal heat

The factors which contribute most to the carbon emissions from constructing and operating a heat-only geothermal project, and the most sensitive factors, are identified and discussed below.

(a) *Land use change*: In this study we have assumed that site development would disturb either arable or heath land. Heath land represents the worst-case scenario for the Banchory region. Emissions would be much higher if the site was developed on peat. The 'best case' scenario would be for development on brown-field sites, for which emissions would be ~negligible. The difference in carbon emissions between these two assumptions is enough to shift the emissions intensity by ~1 kg(CO_2)/MWh$_{th}$. Geothermal energy stations are likely to be sited as close to the end-user as possible to save pipeline cost and losses, and developments will typically be on non-rural brownfield sites. If brownfield site with no modification required for placing

Table 2
Calculated GHG emissions, expressed as CO_2e, for each step of the deep geothermal life cycle assessment for the Banchory Project.

| Activity	Carbon emissions t(CO_{2e})			Direct/indirect emission	Source
	Calculated GHG emissions, expressed	Calculated GHG emissions, expressed	Calculated GHG emissions, expressed		
1. Construction (pre-operation)					
a) Site preparation					
Access roads	60–126				
Pipeline (buried)	280–589				
Well pad	60–126				
Total (land use change)	400–841			Direct	Bond et al. (2014)
Pipeline	63			Indirect	Fröling et al. (2004)
Drill rig transport	15			Direct	NYSDEC (2011)
b) Borehole construction					
Drill rig operation	1243	994	2486	Direct	Bradley (1987)
Drilling fluids/water	10	7.5	20	Indirect	DEFRA (2018)
Well casing	1296	863	1944	Indirect	Yu et al. (2015), WorldSteel (2016)
Borehole cement	360	324	720	Indirect	Salas et al. (2016)
System surface elements (e.g. pump, heat exchanger etc.)	Not calculated			Indirect	
2. Operation (30 year lifetime operating at 60% load)					
Pump rate (min – 14 kW)	419			Indirect	
Pump rate (max – 56 kW)	1678			Indirect	
Total					
Decommissioning	Not calculated				
Total					
Direct CO_2 emissions	1658–2099	1414–1832	2906–3324	Direct	
Indirect CO_2 emissions	2148–3407	1677–2936	3166–4425	Indirect	
Overall	3806–5506	3086–4768	6067–7767		
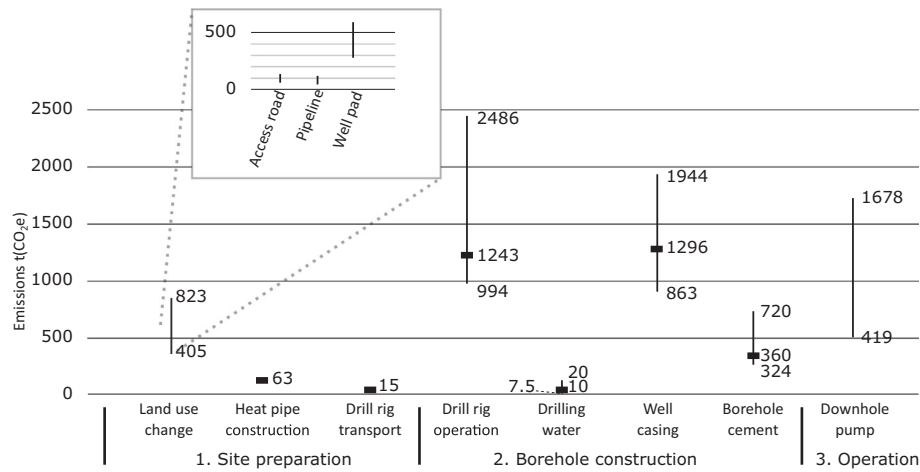
Fig. 4. CO_2e emissions from key activities within the three life cycle stages that we consider in our analysis of the geothermal doublet Banchory Project. The upper and lower bounds for land use change emissions depict whether arable (low carbon) or heath (high carbon) land is disturbed. The graph inset shows the contribution of the three different land clearing activities in the project. Single values are presented for other aspects of site construction. The upper and lower bounds for pump operation depend on assumed power requirements and injection method. Upper and lower bounds for well construction reflect whether the drilling scenario is favourable or challenging (which determines the well depth and drilling time, as well as the quantity of materials needed to line the wellbore).

equipment was assumed, the emissions intensity of the low estimate would reduce to 7 kg(CO_2e)/MWh$_{th}$, a 28% reduction. However a doubling of required land area would result in an increase of the high estimate from 14.0 kg(CO_2e)/MWh$_{th}$ to 15.5 kg (CO_2e)/MWh$_{th}$, a 10.7% increase.

(b) *Drilling conditions*: A drill rig powered by diesel would contribute lifetime emissions intensity of 3 kg(CO_2e)/MWh$_{th}$, or 22–33% of emission intensity. As best practice evolves in response to needs to reduce environmental impact of activities, natural gas or electric powered drill rigs will be used which could lower the emissions intensity of produced heat to 6 kg(CO_2e)/MWh$_{th}$. On the other hand, unplanned issues can significantly extend drilling time. For example, the Science Central geothermal borehole in Newcastle-upon-Tyne (UK) lost a drill bit which required extra drilling (Younger et al., 2016). A 'challenging' conditions scenario with doubled drill time and a greater depth required for the target temperature would lead to an increase in the upper estimate to 19.7 kg(CO_2e)/MWh$_{th}$. On the other hand, favourable drilling conditions have a lower bound estimate of 7.8 kg(CO_2e)/MWh$_{th}$. These emissions of these scenarios are sensitive to drill rig operation, well casing, borehole cement, and consumption of drilling fluids; in that order.

(c) *Depth to the resource*: The emissions produced by drilling the borehole, and the emissions embedded in the system's components depend on the depth of the geothermal resource. If a 10% reduction in depth has a corresponding emissions reduction in the drilling, steel and cement lining, this would result in lowering emission intensity by 0.7 kg(CO_2e)/MWh$_{th}$, 5.2–7.7% of emission intensity. Temperature depth profiles can be uncertain, particularly in an area where no sub-surface data are available. If temperature at depth was significantly underestimated, and required an extra 50% drilling depth then the upper estimate would increase by 1.8 kg(CO_2e)/MWh$_{th}$ to 15.2 kg(CO_2e)/-MWh$_{th}$.

(d) *Surface infrastructure*: Due to a desire to minimise infrastructure costs and heat lost in transportation, geothermal energy stations are likely to be sited as close to the end-user as possible. As such the 1 km of both delivery and return pipe that we assume is extremely conservative. If the distance of pipework is halved, the emissions intensity of the heat would reduce by 0.05 kg(CO_2e)/-MWh$_{th}$, corresponding to 0.5% reduction in emission intensity. This suggests that carbon intensity is insensitive to location of drilling as long as the pipework is not made of a high carbon

solid, and location options should favour minimising drilling and borehole length rather than heat pipe length.

(e) *The quantity of useful heat produced*: Here, we assume that the Banchory project has 2.5 MW$_{th}$ capacity, the site operates at 60% load and that the system provides heat for 30 years. These are generic assumptions. The capacity (2.5 MW$_{th}$) is estimated from the Hill of Fare granite's likely thermal and hydraulic properties. These geological properties are uncertain, and upon drilling the well, it may transpire that the properties of the granite are higher or lower than estimated – and so the quantity of heat that can be sustainably extracted from the granite is higher or lower than anticipated. Similarly, the heat capacity is site dependent, and so will likely differ for other geothermal reservoirs. The heat capacity influences the designed pumping flow rate of the system. If the project capacity (i.e. pump rate and temperature drop of the working fluid), or the operating lifetime is increased, the carbon intensity of the produced heat becomes proportionally reduced, i.e. halving the heat load doubles the carbon intensity for boreholes of the same size. Potentially, geothermal would be best suited to constant industrial or commercial loads in order to minimise national emissions, as compared with electrically powered heat pumps which would have more of their lifecycle emissions due to operations (i.e. the resulting power sector emissions).

(f) *Decline in heat output with time*: If the reservoir underperforms or is otherwise overexploited then heat output may decline over the 30-year lifetime. A heat output decline over the project to 50% of initial rates would mean that the emission intensity is increased to 12.9 to 18.6 kg(CO_2e)/MWh$_{th}$ (a 33% increase).

(g) *Powering the pump*: The largest source of emissions over the 30-year lifetime of the geothermal system source from powering the injection/production pumps. We assume that the pump is powered by grid electricity and it operates at 70% efficiency. Improving the pump efficiency would reduce the heat carbon intensity. Current industry standard pumps are not as efficient as 80%, but there is a strong case for engineered improvements to the efficiency of these pumps, or using alternative low carbon fuel sources. However, as the carbon intensity of grid electricity falls over time, the carbon footprint of operating the pump will also reduce, thus lowering the carbon intensity of geothermal heat. For example, if the project was in a location with access to a power grid with a carbon intensity of 50 kg(CO_2e)/MWh$_e$ for the lifetime of the project, the upper estimate of carbon intensity

of heat produced falls by 3.2 kg(CO_2e)/MWh$_{th}$ (23.8%). Conversely if the available power grid is largely coal-fired and has average emissions of 700 kg(CO_2e)/MWh$_e$ then the upper bound for the geothermal heat emission intensity is 24.8 kg(CO_2e)/MWh$_{th}$ (185% of original upper bound). This is still significantly lower carbon than other options such as natural gas, or heat pumps in a carbon intensive power system.

(h) *Stimulating the granite*: Geothermal wells which prove to have marginal or poor production volumes are occasionally stimulated to increase permeability at the bottom of the borehole and thus increase heat production at the surface (Willems et al., 2017). This procedure uses techniques such as chemical/acid treatments (Portier et al., 2009), thermal stimulation (Grant et al., 2013) or hydraulic fracturing. Hydraulic stimulation for geothermal boreholes is rare (the site selection process, which is usually targeting sedimentary geothermal resource, is usually predicated on avoiding stimulation), and so we do not assume this in our LCA calculations. Knoblauch and Trutnevyte (2018) investigated the trade-off between siting EGS (for combined heat and power) away from populations (due to potential concerns around induced seismicity) or close to populations (in order to effectivity sell the produced heat). For heat-only geothermal, as discussed in this study, siting as close as possible to heat demand is economically essential and pursued in highly populated areas such as Munich (e.g. Dussel et al., 2016) and Paris (e.g. Hamm et al., 2016). If the wells in this study were hydraulically fractured, described by Pratiwi et al. (2018) as a 'worst-case scenario', the carbon intensity of the heat would increase. Pratiwi et al. (2018) do not present the relative contributions of different components to the CO_2e emissions from geothermal well stimulation, but these will source from e.g. the sourcing or manufacture of sand and chemical production for the stimulation fluids, diesel combustion for powering the high-pressure fluid pumps, and transport of surface hardware. Bond et al. (2014) calculated that hydraulic fracturing of shale in the UK would emit approximately 200 t(CO_2e) per well, using similar techniques as that for geothermal stimulation. If both geothermal wells in this study were stimulated using an approach similar to Bond et al. (2014) the carbon intensity of the produced heat would increase by 1 kg(CO_2e)/MWh$_{th}$ (between 7.5 and 10.9%).

The carbon intensity estimates of the modelled geothermal project are most sensitive to a) significant issues with the drilling programme; and b) depth to estimated resource (and therefore the time taken to drill the well). However, even in a worst-case "challenging" scenario where a geothermal well is drilled under challenging conditions the carbon intensity of the resultant geothermal heat remains significantly <10% of the carbon intensity of heat derived from combusting fossil methane.

4.2. Comparison with other studies

Pratiwi et al. (2018) and Karlsdottir et al. (2014) are the most directly comparable studies to our deep geothermal life cycle analysis. However, there are significant differences. Pratiwi et al. (2018) investigated five different scenarios for an enhanced geothermal system in the Upper Rhine Valley, of which one scenario was for heat-only, and assumed that the brines were extracted at 170 °C. This is a relatively high temperature for a heat-only geothermal system. The estimated carbon intensity of the produced heat was 9.15 kg(CO_2)/MWh$_{th}$.

Karlsdottir et al. (2014) presented the case of a geothermally heated district heat network in Iceland. In that case the water production temperature was 70 °C which is similar to the present study. However, this study included the heat network within their estimate of the carbon intensity. Karlsdottir et al. (2014) present an emissions intensity estimate of 5.8 kg(CO_2)/MWh$_{th}$. This is probably quite low because of the favourable geothermal conditions in Iceland which has naturally high geothermal gradient.

Despite the significant differences in scope and geological settings of Karlsdottir et al. (2014) and Pratiwi et al. (2018), the carbon intensity values that they derive are marginally lower than the 9.7–13.4 kg(CO_2)/MWh$_{th}$ that we calculate for the Banchory Project. The estimated emissions from drilling calculate by Pratiwi et al. (2018) are higher than in our study, as the authors assume deeper, more complex drilling. However, the calculated overall emission intensity is lower because they expect the borehole to deliver 180 GWh of heat per year, >10 times the value that we assume for the Banchory Project (13 GWh per year).

Nevertheless, these studies provide useful context for the validity of their approaches and that of this paper, and all three studies agree that direct geothermal heat has very low associated life cycle emissions.

4.3. What are the potential carbon savings over a project lifetime?

The quantity of GHG emissions that could be abated by deep geothermal heat depends on the carbon intensity of the heat that it displaces. The current heat network in Banchory uses wood-chip fuelled biomass, a low carbon fuel. The carbon intensity of biomass is dependent on the fuel variety (wood chip, wood pellets, for example) and on the distance the fuel had been transported. While there is no standard reference figure for the carbon intensity of biomass heat from wood chips, UK forest sourced biomass is estimated to be ~11–17 kg(CO_2e)/MWh$_{th}$ (Bates and Henry, 2009). The carbon intensity of heat from the Banchory heat network can be expected to be the minimum of this range because the fuel used is forestry waste and thinnings from local sources. Thus, we would expect a geothermal well at Banchory to produce heat with a similar carbon footprint to the current biomass derived heat.

However, increasing concerns about air pollution and noise in densely populated areas means that large biomass may be less suited to district heat in towns and cities in the future. 79% of heat networks being developed in the UK are heated by gas-fired combined heat and power (CHP) and boilers (The Association for Decentralised Energy, 2018). 75% of heat supplied to European district heat is directly from fossil fuels or waste heat from fossil fuel power plants (Werner, 2017). As fossil power plants close due to the progressive decarbonisation of power grids, alternative heat sources will be needed. Deep geothermal heat is a low carbon alternative compared with the carbon intensities of gas fired CHP (which raises in intensity as the wider power grid decarbonises) and boilers. Therefore, where deep geothermal replaces natural gas or heating oil heating there is scope for large reductions in carbon emissions.

If we assume that a geothermal system similar to that proposed at Banchory produces 13,140 MWh$_{th}$/Pa and this displaces the same amount of natural gas heating the carbon emissions abated would amount to 2266 t(CO_2e)/Pa (these calculations assume a direct emission intensity of 184.5 kg(CO_2e)/MWh$_{th}$ for natural gas derived heat, based on 100% efficiency of heat transfer in the system). Over the 30-year operational lifetime the geothermal system would save ~68,000 t(CO_2e).

4.4. How much carbon have countries already saved through direct-use geothermal?

The Netherlands is one of the key growth areas for direct-use geothermal in Europe. Geothermal development in the country is supported by comprehensive geological data and government financial de-risking (e.g. dry hole insurance). As of 2015, there were three deep geothermal systems in the Netherlands which produced around 72,000 MWh$_{th}$ annually (Van Heekeren and Bakema, 2015). If such

geothermal projects had carbon intensities calculated in this paper and the geothermal heat displaced natural gas heating they would have saved approximately 13,200 t(CO_{2e}) Pa.

Carbon savings naturally depend on the emission intensity of the technology that is being replaced by geothermal. As an example, in France geothermal heat is primarily exploited in Paris, which makes significant use of the well explored sedimentary basin underlying the city. France produces ~1400 GWh_{th}/Pa of geothermal heat (Vernier et al., 2015). If these geothermal systems displaced natural gas boilers this would result in a carbon saving of 244,000 t(CO_2e) Pa, representing ~0.05% of France's total CO_2 emissions (France emission data viewed at European Environment Agency, 2016). However France has a low power grid emission intensity of 66 kg(CO_2)/MW_e (Moro and Lonza, 2017). If direct geothermal replaced direct electrical heat, then carbon savings would be reduced to 77,000 t(CO_{2e})/Pa. Furthermore, if direct-use geothermal displaced efficient heat pumps with a COP of 3.0 then carbon savings would only be 15,400 t(CO_{2e})/Pa.

China has extensive direct-use geothermal plants with total capacity around 6089 MW_{th} which produce 20,000 GWh_{th}/Pa (Lund and Boyd, 2016). Since the majority of district heat in China has been sourced from coal (Werner, 2017), the emission savings from implementing deep geothermal heat systems will be large. For example, if we assume 320 kg(CO_{2e})/MW_{th} for coal derived heat in China (Hong and Slatick, 1994), and 25 kg(CO_{2e})/MWh_{th} for geothermal heat (owing to a high carbon intensity power grid), the carbon abated by deep geothermal systems is ~5,900,000 t(CO_{2e}) Pa.

Clearly deep geothermal heat offers the greatest emissions reduction when it displaces high emission heat source such as fossil fuel derived sources. We find that using current electrical grid intensity, geothermal heat emits 4.9–7.3% of the emissions compared with natural gas heating in the UK. However, whether direct-use geothermal heat offers carbon intensity low enough to act as a long-term solution (i.e. beyond 2050) depends on the possible future emissions performance requirements for heat and the extent to which system engineering decisions aim to minimise the carbon intensity of heat.

4.5. Is deep geothermal heat compatible with future climate targets?

It is important to consider whether and how deep geothermal heat could play a role in meeting long term carbon emission reduction targets. The Scottish government have committed to a reduction of carbon emissions of 90% (of 1990 levels) by 2050, which is equivalent to an entire carbon budget of 7.6 Mt(CO_{2e}) by 2050. The majority of heat demand in Scotland is met by natural gas supply. In 2015, the natural gas consumption for heat was equivalent to 78,000 GWh, i.e. 14.4 Mt (CO_{2e}) assuming, as before, that the carbon intensity of heat from natural gas is ~184.5 kg(CO_{2e})/MWh_{th}. This represents 25% of the total emissions for Scotland in 2015, and in 2050 would represent almost twice Scotland's entire carbon budget (i.e. for all heating, power, transport, and agriculture etc. needs of the nation).

Across the UK, increasing numbers of district heating and cooling networks powered by natural gas CHP or boilers are being deployed to meet heat demand. While such networks may lower overall emissions compared with previous heat supply (e.g. direct electric or individual boilers), their emissions are not compatible with the UK's long-term climate goals for 2050, and so they offer a stop-gap rather than long-term solution. Although not reasonably feasible, if systems such as the Banchory project met all heat demand in place of natural gas in 2015 (which would require almost 200,000 borehole doublets), our results imply that total CO_{2e} emissions from heat supply would reduce by over an order of magnitude to ~0.7–1.0 Mt(CO_{2e}). These calculations were based on current assumptions. However, in a decarbonised future, a number of life cycle components would reduce in carbon intensity. Firstly, the indirect carbon emissions from operating geothermal heat systems would also be reduced as the carbon intensity of the electricity grid used to power the hydraulic pumps is progressively reduced.

Secondly, it is becoming more common place for drill rigs to be powered by natural gas or electricity, both of which significantly reduce the emissions associated with pre-operation activities, and therefore driving down the carbon intensity of the heat produced. Thirdly, the indirect carbon embedded in raw materials such as steel and cement are expected to decrease as more efficient production measures are developed and put in place. A final consideration is that heat demand will reduce over time as the building stock is replaced or improved and thermal efficiency of buildings is improved. These elements suggest that, in the hypothetical scenario where deep geothermal heat supplies the majority of Scotland's heat, demand in 2050, carbon emissions from heat would constitute <5% of the annual carbon budget.

This suggests that deep geothermal heat could contribute to significant emissions reduction where it is deployed to meet heat demand in place of fossil fuels, and that deep geothermal heat is compatible as part of an ultra-low national energy system. Indeed, where there is a suitable resource, deep geothermal heat systems are well placed to supply district heating when CHP boilers or engines need replaced, in terms of providing appropriately low carbon heat, and re-sing the established district heating infrastructure.

5. Conclusions

We perform a life cycle assessment of greenhouse gas emissions relating to a typical deep geothermal heat system to calculate the carbon intensity of geothermal heat using parameters from a feasibility study for a potential geothermal heat system in Banchory, Scotland. The carbon intensity of geothermal energy projects will inevitably be site specific (due to varying geology, borehole depth, heat capacity, pipeline length and land type), so the presented study is an initial adaptable method that future projects could adapt and apply to assess and enhance the carbon emissions reduction offered by deep geothermal heat projects.

We find that the carbon intensity of deep geothermal heat is in the range 9.7–14.0 kg(CO_{2e})/MWh_{th}. This is over an order of magnitude less than heat from natural gas which meets the majority of current heat demand in the UK.

Favourable drilling conditions lower this estimate to 7.8–12.1 kg (CO_{2e})/MWh_{th}, whereas challenging drilling conditions could raise the estimate to 15.4–19.7 kg(CO_{2e})/MWh_{th}.

The emission intensity of direct heat deep geothermal projects can be reduced significantly by (1) considering low carbon drilling technologies rather than standard diesel power; (2) operating downhole pumps from low carbon electricity sources; and (3) ensuring maximum utilisation of the heat resource once drilled.

Further options for emissions reductions are (1) sourcing low carbon steel and cement, if these options become increasingly available in the future and (2) ensuring emissions from land use change are fully considered in the site appraisal.

Importantly, our analysis shows that deep geothermal heat systems such as the Banchory project can produce very low carbon heat that is compatible with carbon emission reduction targets for 2050 and beyond. Deep geothermal heat systems therefore offer a long-term low carbon option for meeting heat demand into the future.

Geological Survey, Ramboll Energy, Town Rock Energy, and the University of Aberdeen). We hope this paper has built constructively on their original work.

Dr Michael Feliks is grateful for the support from the management and staff of Hotspur Geothermal Ltd for his work on this paper.

The authors are especially grateful for the support and encouragement provided by the late and brilliant Professor Paul L. Younger.

References

Aberdeenshire Council, 2016. Banchory statistics. Available at: https://web.archive.org/web/20160810091732/https://www.aberdeenshire.gov.uk/media/4732/banchoryprofile2014.pdf (Accessed 12 April 2019).

Aksoy, N., Gok, O.S., Mutlu, H., Kilinc, G., 2015. CO2 emission from geothermal power plants in Turkey. Proceedings World Geothermal Congress, p. 2015.

Association for Decentralised Energy, 2018. Market report: heat networks in the UK. Available at: https://www.theade.co.uk/assets/docs/resources/Heat%20Networks%20in%20the%20UK_v5%20web%20single%20pages.pdf (Accessed 24 August 2018).

Bates, J., Henry, S., 2009. Carbon factor for wood fuels for the supplier obligation. DEFRA, London Available at: https://assets.publishing.service.gov.uk/government/uploads/system/uploads/attachment_data/file/48193/3153-final-report-carbon-factor.pdf, Accessed date: 2 September 2018.

BEIS, Department for Business, Energy and Industrial Strategy, 2018. Greenhouse gas reporting conversion factors 2018. Available at: https://www.gov.uk/government/publications/greenhouse-gas-reporting-conversion-factors-2018, Accessed date: 2 September 2018.

Bertani, R., Thain, I., 2002. Geothermal power generating plant CO2 emission survey. vol. 49. IGA News, pp. 1–3.

Bond, C.E., Roberts, J., Hastings, A., Shipton, Z.K., João, E.M., Tabyldy Kyzy, J., Stephenson, M., 2014. Life-cycle assessment of greenhouse gas emissions from unconventional gas in Scotland. ClimateXchange, Edinburgh Available at: https://www.climatexchange.org.uk/research/projects/life-cycle-assessment-of-ghg-emissions-from-unconventional-gas-extraction-in-scotland/, Accessed date: 2 September 2018.

Bradley, H.B., 1987. Petroleum Engineering Handbook. Society of Petroleum Engineers, Richardson.

Bruckner, T., Bashmakov, I.A., Mulugetta, Y., Chum, H., de la Vega Navarro, A., Edmonds, J., Faaij, A., Fungtammasan, B., Garg, A., Hertwich, E., Honnery, D., Infield, D., Kainuma, M., Khennas, S., Kim, S., Nimir, H.B., Riahi, K., Strachan, N., Wiser, R., Zhang, X., 2014. Energy Systems. In: Edenhofer, O., Pichs-Madruga, R., Sokona, Y., Farahani, E., Kadner, S., Seyboth, K., Adler, A., Baum, I., Brunner, S., Eickemeier, P., Kriemann, B., Savolainen, J., Schlömer, S., von Stechow, C., Zwickel, T., Minx, J.C. (Eds.), Climate Change 2014: Mitigation of Climate Change. Contribution of Working Group III to the Fifth Assessment Report of the Intergovernmental Panel on Climate Change. Cambridge University Press, Cambridge, United Kingdom and New York, NY, USA.

Comerford, A., Fraser-Harris, A., Johnson, G., McDermott, C.I., 2018. Controls on geothermal heat recovery from a hot sedimentary aquifer in Guardbridge, Scotland: field measurements, modelling and long term sustainability. Geothermics 76, 125–140.

Committee on Climate Change, 2018. An independent assessment of the UK's Clean Growth Strategy: from ambition to action. Available at: https://www.theccc.org.uk/publication/independent-assessment-uks-clean-growth-strategy-ambition-action/, Accessed date: 2 September 2018.

DECC, Department for Energy and Climate Change, 2012. Emissions from heat: statistical summary. Available at: https://assets.publishing.service.gov.uk/government/uploads/system/uploads/attachment_data/file/140095/4093-emissions-heat-statistical-summary.pdf, Accessed date: 15 June 2018.

DECC, Department for Energy and Climate Change, 2013. Deep geothermal review study: final report. Available. https://www.gov.uk/government/publications/deep-geothermal-review-study, Accessed date: 19 March 2019.

DEFRA, Department for Food, Environment and Rural Affairs, 2018. Government emission conversion factors for greenhouse gas company reporting. Available at: https://www.gov.uk/government/collections/government-conversion-factors-for-company-reporting, Accessed date: 17 August 2018.

Dussel, M., Lüschen, E., Thomas, R., Agemar, T., Fritzer, T., Sieblitz, S., Huber, B., Birner, J., Schulz, R., 2016. Forecast for thermal water use from Upper Jurassic carbonates in the Munich region (South German Molasse Basin). Geothermics 60, 13–30.

EEA, European Environment Agency, 2016. Total greenhouse gas emissions by countries, 1990–2016. Available at: https://ec.europa.eu/eurostat/statistics-explained/index.php?title=File:Total_greenhouse_gas_emissions_by_countries,_1990-2016_(Million_tonnes_of_CO2_equivalents).png, Accessed date: August 2018.

European Commission - Joint Research Centre - Institute for Environment and Sustainability, 2010. Life Cycle Data System (ILCD) Handbook - General Guide for Life Cycle Assessment - Detailed Guidance. First Edition March 2010. EUR 24708 EN. Publications Office of the European Union, Luxembourg.

Forster, D., and Perks, J., 2012, Climate Impact of Potential Shale Gas Production in the EU - Final Report: AEA TEchnology Inc. for EC DG Climate Action, Issue 2.

Frick, S., Kaltschmitt, M., Schröder, G., 2010. Life cycle assessment of geothermal binary power plants using enhanced low-temperature reservoirs. Energy 35 (5), 2281–2294.

Fridriksson, T., Merino, A.M., Orucu, A.Y., Audinet, P., 2017, February. Greenhouse gas emissions from geothermal power production. Proceedings, 42nd Workshop on Geothermal Reservoir Engineering. Stanford University, Stanford, California, pp. 13–15 February.

Fröling, M., Holmgren, C., Svanström, M., 2004. Life cycle assessment of the district heat distribution system. Int. J. Life Cycle Assess. 9 (2), 130–136.

Gluyas, J.G., Adams, C.A., Busby, J.P., Craig, J., Hirst, C., Manning, D.A.C., McCay, A., Narayan, N.S., Robinson, H.L., Watson, S., Westaway, R., 2018. Keeping warm: a review of deep geothermal potential of the UK. Proceedings of the Institution of Mechanical Engineers, Part A: Journal of Power and Energy (p.0957650917749693).

Grant, M.A., Clearwater, J., Quinão, J., Bixley, P.F. and Le Brun, M., 2013, February. Thermal stimulation of geothermal wells: a review of field data. In Proceedings 38th Workshop on Geothermal Reservoir Engineering, Stanford University, Stanford, CA (2013).

Hamm, V., Bouzit, M., Lopez, S., 2016. Assessment of complex well architecture performance for geothermal exploitation of the Paris basin: a modeling and economic analysis. Geothermics 64, 300–313.

Hogarth, R.A., Bour, D., 2015. Flow performance of the Habanero EGS closed loop. Proceedings of World Geothermal Congress 2015. International Geothermal Association, Melbourne.

Hong, B.D., Slatick, E.R., 1994. Carbon dioxide emission factors for coal. Q. Coal Rep. 7, 1–8.

ISO 11960, 2014. 2014 Petroleum and Natural Gas Industries — Steel Pipes for Use as Casing or Tubing for Wells. International Organization for Standardization, Geneva, Switzerland.

Karlsdottir, M.R., Lew, J.B., Palsson, H.P., Palsson, O.P., 2014. Geothermal district heating system in Iceland: a life cycle perspective with focus on primary energy efficiency and CO2 emissions. The 14th International Symposium on District Heating and Cooling, 2014.

King, G.E., 2012. Hydraulic fracturing 101: what every representative, environmentalist, regulator, reporter, investor, university researcher, neighbor, and engineer should know about hydraulic fracturing risk. J. Pet. Technol. 64 (04), 34–42.

Knoblauch, T.A., Trutnevyte, E., 2018. Siting enhanced geothermal systems (EGS): heat benefits versus induced seismicity risks from an investor and societal perspective. Energy 164, 1311–1325.

Lund, J.W., Boyd, T.L., 2016. Direct utilization of geothermal energy 2015 worldwide review. Geothermics 60, 66–93.

MacKay, D., Stone, T., 2013. Potential Greenhouse Gas Emissions Associated With Shale Gas Production and Use. Department of Energy & Climate Change (DECC).

McCay, A.T., Younger, P.L., 2017. Ranking the geothermal potential of radiothermal granites in Scotland: are any others as hot as the Cairngorms? Scott. J. Geol. 53, 1–11.

Milligan, G., Wood, G., Younger, P., Feliks, M., McCay, A., Gillespie, M., Steen, P., McBeth, N., Townsend, D., Townsend, P., Stephenson, R., Gomez-Rivas, E., 2016. Hill of Banchory Geothermal Energy Project feasibility study report. Scottish Government Available at. http://www.gov.scot/Publications/2016/03/6881, Accessed date: 2 September 2018.

Moro, A., Lonza, L., 2017. Electricity carbon intensity in European Member States: impacts on GHG emissions of electric vehicles. Transp. Res. Part D: Transp. Environ. 64, 5–14.

Nayak, D.R., Miller, D., Nolan, A., Smith, P., Smith, J.U., 2010. Calculating carbon budgets of wind farms on Scottish peatlands. Mires Peat 4 (9), 1–23 (April 29).

Ng'ang'a, S.I., 2014. Cementing processes in geothermal well drilling: application and techniques. KenGen Report, No. 23. UNU-Geotheraml Training Programme, Reykavic Available at: https://orkustofnun.is/gogn/unu-gtp-report/UNU-GTP-2014-23.pdf, Accessed date: 2 September 2018.

NYSDEC, New York State Department of Environmental Conservation, 2011. Supplemental generic environmental impact statement on the oil, gas and solution mining regulatory programme: well permit issuance for horizontal drilling and high-volume fracturing to develop the Marcellus Shale and other low-permeability gas reservoirs. Available at: http://www.dec.ny.gov/data/dmn/rdsgeisfull0911.pdf, Accessed date: 2 September 2018.

Oertel, C., Matschullat, J., Zurba, K., Zimmermann, F., Erasmi, S., 2016. Greenhouse gas emissions from soils—a review. Chem. Erde-Geochem. 76 (3), 327–352.

Ofgem, 2014. Non Domestic Renewable Heat Incentive Guidance Volume One: Version 5 (2014).

Portier, S., Vuataz, F.D., Nami, P., Sanjuan, B., Gérard, A., 2009. Chemical stimulation techniques for geothermal wells: experiments on the three-well EGS system at Soultz-sous-Forêts, France. Geothermics 38 (4), 349–359.

Pratiwi, A., Ravier, G., Genter, A., 2018. Life-cycle climate-change impact assessment of enhanced geothermal system plants in the Upper Rhine Valley. Geothermics 75, 26–39.

Ryan, T., Phillips, H., Ramsay, J., Dempsey, J., 2004. Forest Road Manual. Guidelines for the Design, Instruction and Management of Forest Roads. COFORD, Dublin Available at. https://www.unirc.it/documentazione/materiale_didattico/598_2007_39_832.pdf, Accessed date: 14 June 2018.

Salas, D.A., Ramirez, A.D., Rodríguez, C.R., Petroche, D.M., Boero, A.J., Duque-Rivera, J., 2016. Environmental impacts, life cycle assessment and potential improvement measures for cement production: a literature review. J. Clean. Prod. 113, 114–122. https://doi.org/10.1016/j.jclepro.2015.11.078.

Scheiber, J., Seibt, A., Birner, J., Genter, A., Moeckes, W., 2013. Application of a scaling inhibitor system at the geothermal power plant in soultz-sous-Forêts: laboratory and on-site studies. Proceedings European Geothermal Congress June.

Scottish Government, 2018. Energy in Scotland 2018. Available at: https://www.gov.scot/Resource/0053/00531701.pdf, Accessed date: 18 July 2018.

SEPA, Scottish Environmental Protection Agency, 2012. Regulatory guidance: coal bed methane and shale gas. Currently unavailable to due national moratorium (02 September 2018).

Sullivan, J.L., Burnham, A., Wang, M., 2010. Energy-consumption and Carbon-emission Analysis of Vehicle and Component Manufacturing (No. ANL/ESD/10-6). Argonne National Lab.(ANL), Argonne, IL (United States).

Tavman, I., Kumlutas, D., Tavman, Ş., 2005. Low enthalpy geothermal energy utilization for greenhouse heating in the Aegean Region of Turkey. World Geothermal Congress.

UK Soil Observatory, 2007. http://www.ukso.org/home.html, Accessed date: 12 April 2019.

United Nations Framework Convention on Climate Change, 2015. Adoption of the Paris Agreement, 21st Conference of the Parties. United Nations, Paris Available at. https://unfccc.int/process-and-meetings/the-paris-agreement/the-paris-agreement, Accessed date: 2 September 2018.

Van Heekeren, V., Bakema, G., 2015. The Netherlands country update on geothermal energy. Proceedings World Geothermal Congress 2015. International Geothermal Association, Melbourne, pp. 19–24.

Vernier, R., Laplaige, P., Desplan, A., Boissavy, C., 2015. France country update. Proceedings to World Geothermal Congress. International Geothermal Association, Melbourne April.

Ward, S.E., Smart, S.M., Quirk, H., Tallowin, J.R., Mortimer, S.R., Shiel, R.S., Wilby, A., Bardgett, R.D., 2016. Legacy effects of grassland management on soil carbon to depth. Glob. Chang. Biol. 22, 2929–2938. https://doi.org/10.1111/gcb.13246.

Werner, S., 2017. International review of district heating and cooling. Energy 137, 617–631. https://doi.org/10.1016/j.energy.2017.04.045.

Willems, C.J., Nick, H.M., Donselaar, M.E., Weltje, G.J., Bruhn, D.F., 2017. On the connectivity anisotropy in fluvial Hot Sedimentary Aquifers and its influence on geothermal doublet performance. Geothermics 65, 222–233.

WorldSteel, 2016. Sustainability Indicators: Definitions, Relevance and Data 2003–2015. vol. 137. World Steel Association, pp. 617–631.

Younger, P.L., Manning, D.A., 2010. Hyper-permeable granite: lessons from test-pumping in the Eastgate Geothermal Borehole, Weardale, UK. Q. J. Eng. Geol. Hydrogeol. 43 (1), 5–10. https://doi.org/10.1144/1470-9236/08-085.

Younger, P.L., Manning, D.A., Millward, D., Busby, J.P., Jones, C.R., Gluyas, J.G., 2016. Geothermal exploration in the Fell Sandstone Formation (Mississippian) beneath the city centre of Newcastle upon Tyne, UK: the Newcastle Science Central deep geothermal borehole. Q. J. Eng. Geol. Hydrogeol. 49 (4), 350–363.

Yu, B., Li, X., Qiao, Y., Shi, L., 2015. Low-carbon transition of iron and steel industry in China: carbon intensity, economic growth and policy intervention. J. Environ. Sci. 28, 137–147.